Localization and quantum Hall effect in a two-dimensional periodic potential

1994 J. Phys.: Condens. Matter 6 7941

(http://iopscience.iop.org/0953-8984/6/39/015)

J. Phys.: Condens. Matter 6 (1994) 7941–7954. Printed in the UK

Localization and quantum Hall effect in a two-dimensional periodic potential

Yong Tan†
Department of Physics FM-15, University of Washington, Seattle, Washington 98195, USA

Received 9 May 1994, in final form 7 July 1994

Abstract. A numerical study has been made of two-dimensional electrons in the lowest Landau level in the presence of a periodic potential and a random potential. The Hall conductance, density of states and density of current-carrying states are calculated when disorder is varied. The results show that the states in a subband carrying quantized Hall conductance t ($t > 1$ for example, and similarly $t < -1$) are split into two carrying unit conductance and $t - 1$, respectively, as disorder is introduced. The states carrying unit Hall current will merge and annihilate with that carrying -1 in the neighbouring subband separated by a small gap when disorder is increased and the gap vanishes. Based on this, a diagram of current-carrying states against disorder has been proposed. There is also a calculation on the localization length, and it is found that extended states appear at singular energies under certain conditions. Futhermore, it has been shown that a plateau in the Hall conductance, rather than a rapid oscillation, can be measured as a function of magnetic field for one-third-filled Landau bands. Similar results have been obtained for tight-binding electrons in a magnetic field with random site energies.

1. Introduction

The discovery of the integer quantum Hall effect [1] in otherwise totally localized [2] two-dimensional disordered electron systems indicates the coexistence of both extended and localized states in a magnetic field [3]. Various studies, including percolation theory [4, 5], one-parameter scaling theory [6–8] and calculation of Thouless number [9], have been made of the nature of the localization in Landau levels. It is generally believed that the localization length diverges at the centre of Landau levels as a power law [4–9]. Meanwhile, the quantization of the Hall conductance has been found to be of topological origin [10–13]. This was further exploited to show that the topology of the wavefunction can be used as a probe to distinguish between localized and extended states [14]. Based on this, numerical calculations [15] have yielded an exponent of the localization length in good agreement with the analytical prediction [5].

A natural extension is to split Landau levels, as could arise in the presence of weak periodic potentials. This, on its own, is very interesting because it generates the commensurability problem with several competing length scales involved. A two-dimensional cosine potential is known to give the Harper equation [16] and its Hofstadter spectrum [17], which have been extensively studied. The Hall conductance of the subbands has been obtained explicitly in terms of solutions of the Diophantine equation [10, 18]. Of course, the formulation leading to the topological explanation for the quantum Hall effect

† Current address: Department of Physics and Applied Physics, John Anderson Building, University of Strathclyde, Glasgow G4 0NG, UK.

0953-8984/94/397941+14$19.50

was originally made in this system [10]. In the limit of tight-binding electrons in a magnetic field with random site energies, Ando has calculated the localization length numerically [19] by the Thouless number [20, 21], and has obtained the Hall conductance [22].

Recently, several experiments seem to indicate the possible realization of the Hofstadter spectrum [23–25]. Lateral superlattices have been generated in high-mobility GaAs/AlGaAs heterostructure samples. The period of the superlattice is typically about 300 nm, so a magnetic field of a few tesla is able to give a magnetic flux in each unit cell of the same order as the flux quantum. Therefore the splitting of Landau levels can be resolved experimentally. It has been shown [24, 26, 27] that the band splitting has to be taken into account in order to understand the experimental measurements on the longitudinal resistance [23, 24].

The band splitting, however, can be demonstrated more directly in the Hall conductance. The usual plateau in the Hall conductance will be replaced by some fine structures if the Landau level is split. In this paper, the possible shape of these fine structures is investigated. First of all, disorder should be considered in a real experimental sample. Therefore the Hofstadter spectrum will be modified accordingly. In section 2, the general formulation of this numerical calculation will be presented. The method used to calculate Hall conductance follows that of Thouless *et al* [10, 28]. This study is focused on how the inclusion of disorder affects the result obtained by Thouless *et al* [10] and Středa [18]. The distribution of the Hall conductance in the split Landau levels has been calculated for two fractions of the flux. It has been shown that the gaps vanish as disorder is increased, and the Hall currents carried by a subband split, merge and annihilate with others. This results, for sufficiently strong disorder, in a broadened Landau band where no band splitting occurs and the Hall current is carried at the centre.

In section 3, the possible experimental outcome for the Hall conductance has been studied. It is shown that, taking localization into account, a plateau can be measured as a function of magnetic field for one-third filling of the Landau level. The localization length has been obtained by the Thouless number method. In section 4, similar conclusions are drawn for the tight-binding electrons. Moreover, it can be concluded that the Hall current is still carried by a singular energy in a subband if the Hall conductance is either 1 or -1. However, a doubt remains if a subband carries a higher Hall current or there is a $(1, -1)$ pair present, where the possibility of mobility edges exists.

The above results are summarized in section 5, where a qualitative phase diagram of the current-carrying states is proposed as a function of disorder.

2. Split Landau levels

2.1. General formulation

The system studied in this paper is a two-dimensional non-interacting electron gas which is subject to a uniform magnetic field and modulated by a weak periodic potential. Rectangular geometry is assumed for the periodic modulation; it is possible to generalize the results, at least numerically, to other geometries. This defines a unit cell of $a \times b$. The magnetic field is perpendicular, and the magnetic flux through each unit cell is given by

$$Bab = (p/q)\phi_0 \tag{2.1}$$

where $\phi_0 = h/e$ is the flux quantum, and p, q are mutually primed integers. The magnetic unit cell is defined as $qa \times b$, such that an integer number of flux quanta are included. In

general, one needs to consider longer periods, L_1 and L_2, than the magnetic unit cell. This becomes necessary in the presence of disorder. However, L_1 and L_2 should be commensurate with the magnetic unit cell, namely,

$$L_1 = qaM_1 \qquad L_2 = bM_2 \tag{2.2}$$

where M_1, M_2 are integers.

2.1.1. Projection onto Landau levels. In the limit of strong magnetic fields, the Hamiltonian can be projected onto the Landau levels $|N, X\rangle$, explicitly,

$$H = \sum_{N,X} |N, X\rangle E_N \langle N, X| + \sum_{N,X} \sum_{N',X'} |N', X'\rangle \langle N', X'|V|N, X\rangle \langle N, X| \tag{2.3}$$

where $E_N = (N + \frac{1}{2})\hbar\omega_c$, with the Landau level index N and the cyclotron frequency ω_c. The potential V consists of the periodic modulation V_p and the disorder potential V_d. The guiding centre is reflected in the variable X, which is expressed in terms of a set of integers, $X = (s, n, j)$. The definition of these integers is implied in equation (2.5). The wavefunction $|N, X\rangle$ can be constructed by the usual Landau wavefunctions $\chi_N(x)$, explicitly [10],

$$\psi_{N,X,k}(x, y) = \exp(ik_1 x + ik_2 y) f_{N,X,k}(x, y) \tag{2.4}$$

where

$$f_{N,X,k}(x, y) = L_2^{-1/2} \sum_{t=-\infty}^{\infty} \chi_N(x - R - l^2 k_2) \exp[-ik_1(x - R) + iyR/l^2] \tag{2.5a}$$

and

$$R = tL_1 + sqa + nqa/p + 2\pi l^2 j/L_2 \tag{2.5b}$$

with the magnetic length l and the wavenumber $k = (k_1, k_2)$. It is obvious in equation (2.5) that these integers are bound by $0 \leqslant s \leqslant M_1 - 1$, $1 \leqslant n \leqslant p$ and $0 \leqslant j \leqslant M_2 - 1$.

The boundary conditions can be obtained by magnetic translation. Equations (2.4) and (2.5) give

$$\begin{aligned} \psi_{N,X,k}(x + L_1, y) &= \exp(iL_1 y/l^2 + ik_1 L_1)\psi_{N,X,k}(x, y) \\ \psi_{N,X,k}(x, y + L_2) &= \exp(ik_2 L_2)\psi_{N,X,k}(x, y). \end{aligned} \tag{2.6}$$

Therefore the boundary of the unit cell in k-space is given by $0 \leqslant k_1 \leqslant 2\pi/L_1$ and $0 \leqslant k_2 \leqslant 2\pi/L_2$.

Assuming that the modulation and disorder are weak, $|V_p|, |V_d| \ll \hbar\omega$, interaction between Landau levels can be ignored. The effect of the periodic and disorder potentials is taken into account by using perturbation theory. Consider a specific modulation potential

$$V_p(x, y) = V_0 \cos(2\pi x/a) + V_0' \cos(2\pi y/b). \tag{2.7}$$

This gives the matrix elements

$$\begin{aligned}\langle N, X'|V_p|N, X\rangle &= V'\exp(-iqak_1/p)\delta_{sp+n,s'p+n'-1}\delta_{j,j'} \\ &+ 2V\cos(2\pi nq/p + 2\pi qj/pM_2 + qbk_2/p)\delta_{n,n'}\delta_{s,s'}\delta_{j,j'} \\ &+ V'\exp(iqak_1/p)\delta_{sp+n,s'p+n'+1}\delta_{j,j'} \qquad (2.8)\end{aligned}$$

where $V = 0.5V_0\exp(-\pi^2l^2/a^2)L_N(2\pi^2l^2/a^2)$, and $L_N(x)$ is the Laguerre polynomial. V' can be obtained similarly. This is the Harper equation [16], where the fact that the size is larger than the magnetic unit cell has been taken into account. There are p bands appearing in the energy spectrum. Diagonalization of equation (2.8) gives pM_1M_2 subbands, but M_1M_2 subbands touch or overlap with each other, and can actually be considered as one distinguishable band. In addition, if M_2 is commensurate with q, there are q subbands completely degenerate. In other words, they overlap entirely in the k-space. This degeneracy will be lifted in the presence of disorder potentials.

The disorder is introduced by randomly placed short-range scatterers. For simplicity, δ-type potentials are chosen, namely [9]

$$V_d(x, y) = \sum_i U\delta(r - r_i) \qquad (2.9)$$

where $U = \pm V_1$, and r_i are the random sites of the scatterers. The numbers of positive and negative scatterers are chosen to be equal. Moreover, the disorder potential V_d is chosen to be periodic, with periods L_1 and L_2 in the x and y directions, respectively. This reduces the Hamiltonian to a finite-size matrix. It has been shown [9] that the zeros of the wavefunction can be adjusted to coincide with the locations of the scatterers if the concentration of the scatterers is low. Thus disorder involves no change in the energy. Therefore the scatterers have to be dense in order to be effective. In this calculation, the averaged space between scatterers is set to be shorter than the magnetic length.

2.1.2. Calculation of Hall conductance. The Hall conductance can be calculated by using the Kubo formula. When equation (2.4) is plugged into the corresponding Schrödinger equation, the Hamiltonian can be rewritten such that its solution becomes $f_{N,X,k}$ rather than $\psi_{N,X,k}$. Therefore the velocity operator can be expressed properly as the partial derivative of the Hamiltonian with respect to the wavenumbers k_1 and k_2. Then the use of the first-order perturbation theory leads to the Hall conductance given by [10–12]

$$\sigma_H = \frac{ie^2}{2\pi h}\sum\int d^2k\int d^2r\left(\frac{\partial u^*}{\partial k_1}\frac{\partial u}{\partial k_2} - \frac{\partial u^*}{\partial k_2}\frac{\partial u}{\partial k_1}\right) \qquad (2.10)$$

where the sum runs over all the occupied states. The wavefunction u is $\sum_X f_{N,X,k}$ in the absence of periodic and disorder potentials. However, in general, one needs to diagonalize the Hamiltonian, equation (2.3), which is a finite $pM_1M_2 \times pM_1M_2$ matrix. Therefore the wavefunction u is written as

$$u_k^i(x, y) = \sum_X d_X^i(k_1, k_2)f_{X,k}(x, y) \qquad (2.11)$$

where the coefficient d_X^i is the eigenvector of the ith eigenvalue. Here the Landau level index N is omitted since only the lowest Landau level is considered in a sufficiently strong magnetic field.

The integral equation (2.10) defines the first Chern class of a U(1) principal fibre bundle of the ground-state wavefunctions on a torus. It gives necessarily an integer multiple of e^2/h. The contributions of d_X^i and $f_{X,k}$ can be evaluated separately. This basis function $f_{X,k}$ gives the Hall conductance of unity in the unit of e^2/h, which, however, will be split equally to each of the pM_1M_2 subbands, namely $1/pM_1M_2$ for each subband, when the periodic and disorder potentials split the Landau level.

To obtain the contribution of the coefficient d_X^i, equation (2.10) is used where the function u is $d_X^i(k_1, k_2)$ instead. The spatial integration over (x, y) must also be replaced by summation over X. The integral over the k-space unit cell can be converted to a contour integral around its boundary. The total phase change of the wavefunction along this contour has been shown to give the Hall conductance.

Now let us separate the modulus and the phase of d_X^i, and consequently write

$$d_X^i(k_1, k_2) = |d_X^i(k_1, k_2)| \exp[i\theta_X^i(k_1, k_2)]. \tag{2.12}$$

The structure of d_X^i in the k-space can be found easily. As k_1 is changed by $2\pi/L_1$, the energy and the modulus of the wavefunction remain the same, while the phase θ_X^i may be different. When k_2 is changed by $2\pi/L_2$, the X component of the modulus can also return, but to a different site X'. It can be shown from equation (2.5) that $X = (s, n, j)$ goes to $X' = (s, n, j + 1)$. Therefore the total phase change for the closed contour is given by

$$\Delta\theta_i = \theta_{X'}^i(2\pi/L_1, 2\pi/L_2) - \theta_{X'}^i(0, 2\pi/L_2) - \theta_X^i(2\pi/L_1, 0) + \theta_X^i(0, 0) \tag{2.13}$$

which is independent of X. However, an overall arbitrary phase of the wavefunction involves no change in the system. To solve this, two conditions have been imposed [28], explicitly

$$\begin{aligned} &\sum_X d_X^i(k_1, 0)^* \frac{\partial}{\partial k_1} d_X^i(k_1, 0) = 0 \\ &\sum_X d_X^i(k_1, k_2)^* \frac{\partial}{\partial k_2} d_X^i(k_1, k_2) = 0. \end{aligned} \tag{2.14}$$

This leaves three legs of the contour zero but the one $k_2 = 2\pi/L_2$, $0 \leqslant k_1 \leqslant 2\pi/L_1$, and the phase $\theta_X^i(k_1, k_2)$ can be uniquely determined. Numerical calculations have been performed on $N \times N$ mesh points in the k-plane, where N is large enough that the missing of a phase of 2π can be avoided. It can be shown that the Hall conductance of d_X^i, given by $\Delta\theta_i/2\pi$, is an integer minus $1/pM_1M_2$ for each subband.

2.1.3. Diophantine equation and its application. In the absence of disorder, the Hall conductance of the rth band has been found to be $(t_r - t_{r-1})$, where t_r can be determined by the Diophantine equation [10, 18]

$$s_r q + t_r p = r \tag{2.15}$$

with $|s_r| \leqslant \frac{1}{2}p$. As disorder is introduced, q degenerate subbands of the rth band will separate in the k-space, though they may still overlap in the energy space with each other, or with the rest of the M_1M_2 subbands. Some of the M_1M_2 subbands will carry quantized Hall currents, but the total Hall current remains $(t_r - t_{r-1})$ if this band is separated from others by gaps. This certainly provides a criterion that the numerical results should satisfy.

2.2. *Flux* $\phi = \frac{3}{2}$

Figure 1 shows the numerical results for a typical sample, where the magnetic field is given by $p/q = \frac{3}{2}$. This is the simplest fraction of q/p which reveals interesting features of the Hall conductance, because other bands besides the central one also carry Hall currents. Without disorder, three bands in the Hofstadter spectrum carry the Hall current $(1, -1, 1)$, respectively. In this calculation, square symmetry has been used where $V = V'$ and $a = b$. L_1 and L_2 are chosen to be $4a$, so it is made of eight magnetic unit cells and consequently gives 24 subbands. The degree of disorder is characterized by the ratio V_1/V for a fixed concentration of scatterers. Four cases with $V_1/V = 0.2,\ 0.4,\ 0.6$ and 0.8 have been computed while the configuration of the random scatterers remains the same.

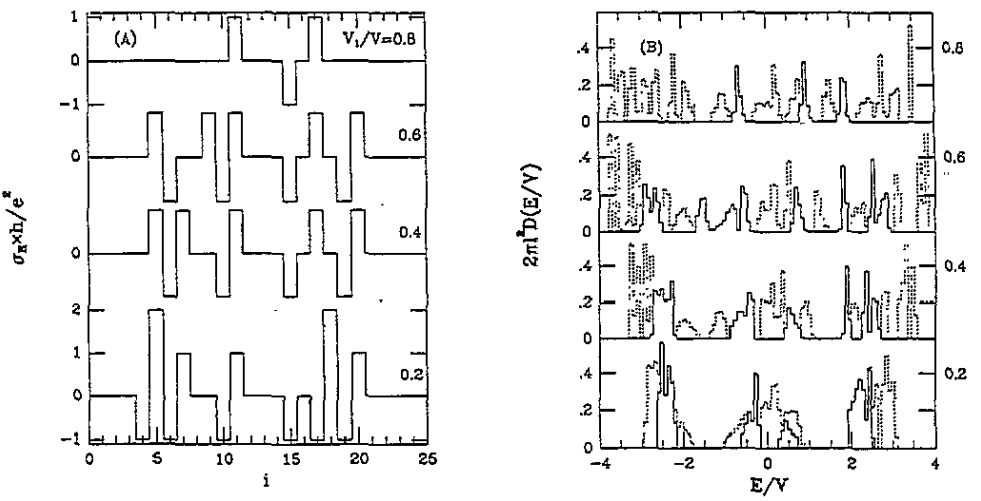

Figure 1. The calculated Hall conductance for one sample is plotted in (A) against the subband index i. Four values of $V_1/V = 0.2, 0.4,\ 0.6$ and 0.8 are calculated for $q/p = \frac{2}{3}$. The corresponding density of states (dotted line), and density of current-carrying states (full line) can be found in (B) as a function of rescaled energy E/V. The total density is one particle per $2\pi l^2$ area.

The calculated Hall conductance is plotted in figure 1(A). It is precisely quantized for each subband. For weak disorder, such as $V_1/V = 0.2$, the criterion mentioned earlier is satisfied. For example, the first eight subbands, which actually form one band and are separated from others by a gap, carry the total of one Hall current. One notices that the Hall currents in one band are widely distributed in its subbands. Therefore it is necessary to locate these subbands in the energy space. This can be depicted explicitly by the density of states [15], which is calculated by counting the number of eigenvalues in an energy interval. The *current-carrying states* are identified to be those subbands whose Hall conductance is different from zero. The density of states for each subband is calculated, and the total density of states at a given energy is obtained by adding the contributions from all subbands. To obtain the density of current-carrying states, this summation is carried out with a weight which is unity for current-carrying subbands and zero otherwise. The results are shown in figure 1(B) where the total density is normalized to $1/2\pi l^2$. Though the Hall currents are carried by several subbands, they may not be distinguishable in the energy space. As

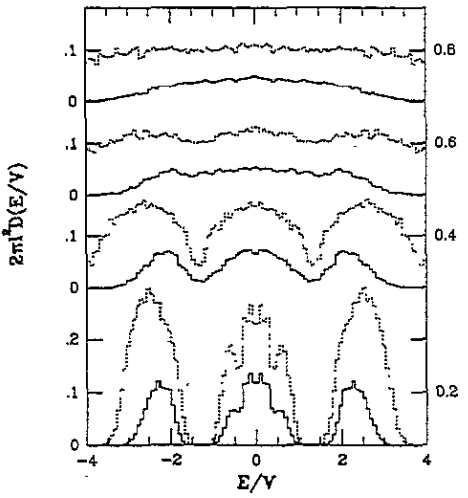

Figure 2. The histogram of the sample averaged density of states (dotted line) and density of current-carrying states (full line) is shown for $q/p = \frac{2}{3}$. The numbers on the right-hand side give the values of V_1/V.

disorder increases, some current-carrying states merge and annihilate with those carrying currents of opposite sign.

The distribution of the Hall currents depends strongly on the configuration of the scatterers. In general, the current-carrying states can appear anywhere in energy space, but, of course, with a probability which is determined by the size of the system and localization length. It is most probable for them to appear at certain energies, while the probability of being elsewhere is exponentially small. To locate these energies, the average over different configurations needs to be taken for the same V_1/V. 65 samples have been calculated, and for each sample there is also a calculation when the sign of all the scatterers is reversed. However, this does not necessarily give the same results as simply changing the sign of the energy E from previous calculations. One needs to further shift all the scatterers coherently by a displacement of $(\frac{1}{2}a, \frac{1}{2}b)$. This effectively reverses the sign of the periodic potential. Therefore the averaged density of states is symmetric about $E = 0$. The dotted line is the density of states, and the full line represents the current-carrying states in figure 2. It is demonstrated that, as disorder is increased, the gaps shrink and finally vanish. Meanwhile, two current-carrying states in the lower and upper bands move closer to the central one. For a particular degree of disorder, three current-carrying states merge together at the centre of the spectrum. This gives a resultant Hall conductance of unity, as is expected since one can ignore the periodic potential in a strong-disorder potential.

2.3. *Flux* $\phi = \frac{5}{3}$

Let us then consider $q/p = \frac{3}{5}$. Equation (2.15) gives the Hall currents $(-1, 2, -1, 2, -1)$ for five bands, respectively. The calculation is made where $L_1 = L_2 = 3a$. The Hall conductance is plotted in figure 3(A) for eight values of V_1/V. The corresponding density of current-carrying states is shown in figure 3(B). As disorder increases, the current-carrying states in the second band, or similarly in the fourth band as well, split into two, each of which carries one Hall conductance. Then one of them and the current-carrying states in the first band, or the fifth band, respectively, where the Hall current of -1 appears, move towards each other. The $(1, -1)$ pairs are formed, which disappear finally if one further increases the disorder. For a certain degree of disorder, for example $V_1/V = 0.2$ in this sample, the resultant spectrum is similar to that of $q/p = \frac{2}{3}$. The smaller gaps have

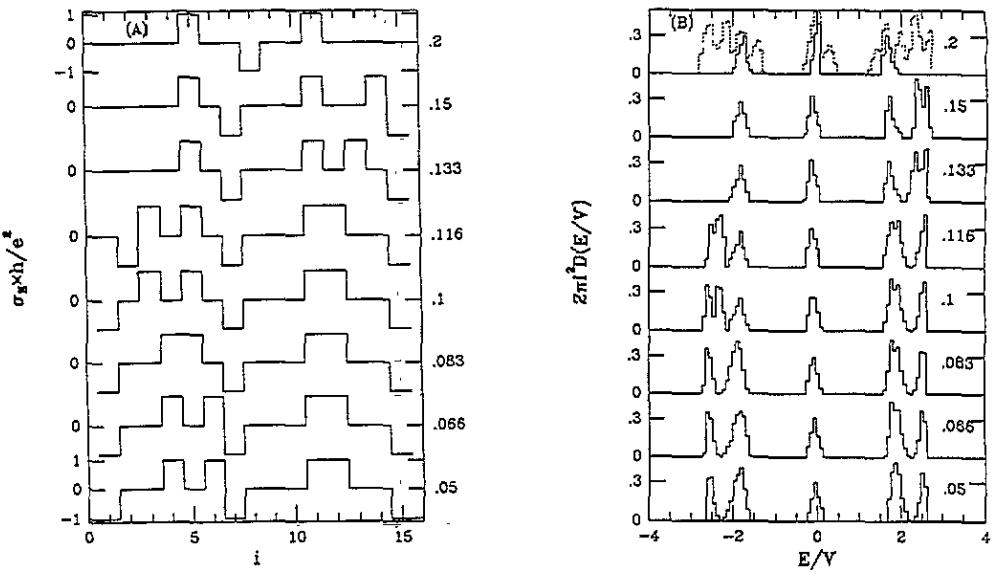

Figure 3. The calculated Hall conductance for one sample is plotted in (A) against the subband index i. The numbers on the right-hand side give eight values of V_1/V for $q/p = \frac{3}{2}$. Figure 3(B) draws the corresponding density of current-carrying states (full line). The total density of states is also drawn (dotted line) for $V_1/V = 0.2$ in (B).

vanished and there are three bands separated by two gaps. They carry the Hall currents of $(1, -1, 1)$, respectively.

3. Hall conductance at fixed filling

If the Hofstadter spectrum is resolved in high-mobility samples, there is no doubt that a plateau structure can be measured as a function of Fermi energy, or carrier concentration, for a fixed magnetic magnetic field [10]. However, it seems much easier experimentally to vary the magnetic field rather than the carrier concentration. It is not so obvious that a plateau can still be observed as a function of magnetic field. This is certainly unlikely if there is no disorder. Specifically, consider a fixed filling factor $\nu = \frac{1}{3}$. If one starts with a magnetic field at $p/q = \frac{3}{2}$, the Fermi energy lies in the gap between the lower and central bands. This gives a quantized Hall conductance of one (e^2/h). Let us then increase the magnetic field to $p/q = \frac{5}{3}$. The Fermi energy now lies in the second band and the measured Hall conductance is not quantized. In fact, while the magnetic field is increased, the band structure changes in a very complicated way according to the flux [17]. Consequently, this results in a rapid oscillation in the Hall conductance at the Fermi energy.

The situation may, however, be different if disorder is present. Fine structures characterized by small gaps in the Hofstadter spectrum will no longer exist. The current-carrying states will be rearranged according to the rules described in the last section. Take $p/q = \frac{5}{3}$ for example. The total density of states is drawn in figure 3(B) for $V_1/V = 0.2$. The localized states, which are identified as those which do not carry Hall currents, can be found on both sides of the gaps. To avoid sample fluctuation, the averaged density of states and the density of the current-carrying states have been calculated. As shown in figure 4,

the current-carrying states peak at the energy $E_c = 0, \pm 1.88$, but spread over the entire band. The Fermi energy lies at $E = -1.72$ for a filling of $\nu = \frac{1}{3}$. It can be concluded that the measured Hall conductance is quantized only if a singular energy in each band carries the Hall current, in analogy to the usual integer quantum Hall effect. It is necessary to investigate the localization in this system.

There are many ways to study the localization. One approach is to observe whether the peak of the current-carrying states shrinks when L_1 and L_2 become larger [15], but this has not been pursued in this paper. Instead, the Thouless number method [9, 19–21] has been used to estimate directly the localization length $\xi(E)$. This method has great advantages for carrying out numerical calculations since only the eigenvalues are needed. The Thouless number is defined in the form

$$g(L) = L^2 D(E) \overline{\Delta E} \sim \exp[-L/\xi(E)] \tag{3.1}$$

where it is assumed that $L_1 = L_2 = L$. $D(E)$ is the density of states, and the inverse of $L^2 D(E)$ measures the level spacing. $\overline{\Delta E}$ is the shift of an energy level due to the change in boundary conditions. Specifically, while keeping the periodic boundary condition in the x direction, namely $k_1 = 0$, the energy shift is obtained from the eigenvalues satisfying periodic ($k_2 = 0$) and antiperiodic ($k_2 = \pi/L_2$) boundary conditions in the y direction, respectively. To avoid sample fluctuation, the geometric average of $\overline{\Delta E}$ has been taken over different samples. For two-dimensional systems, $g(L)$ falls off exponentially with respect to L in the localization regime and remains constant for extended states. To estimate the localization length, two sizes with $L = 6a$ and $9a$ have been calculated.

The results are shown in figure 4, where the inverse localization length indeed approaches zero at singular energies $E_c = 0, \pm 1.80$. These energies shift slightly from the values obtained previously. It is possible that this method gives an effectively larger value of V_1/V than the previous one by comparing their density of states. However, this does not affect the conclusion that the Hall currents are carried at some particular energies. The locations of these energies obtained by the previous method are more accurate, since the wavenumbers have been integrated. Furthermore, there exist local minima at $E = \pm 2.36$, and correspondingly secondary peaks at $E = \pm 2.44$, in the density of current-carrying states. This is where a $(1, -1)$ pair is just annihilated, and the extended states there turn out to be localized.

One expects similar features for the fractions between $q/p = \frac{2}{3}$ and $\frac{3}{5}$. Disorder smears out smaller gaps and one Hall current is carried at a particular energy. Therefore, if the filling is fixed at $\nu = \frac{1}{3}$ and the magnetic field is increased from $q/p = \frac{2}{3}$ to $\frac{3}{5}$, the Fermi energy always lies in the localized regime. This certainly suggests a plateau in the measurement. It is essential that the strength of disorder fits the requirement. Too much disorder will destroy the whole structure. If disorder is too weak, the Fermi energy may be located in the extended regime.

4. Tight-binding electrons

In the opposite limit where the lattice potential dominates, the system is well described by the tight-binding model. It is possible to realize this model experimentally in a sample modulated by antidots. The Hamiltonian can be written as [19, 22]

$$H = \sum_i \epsilon_i c_i^\dagger c_i + \sum_{\langle ij \rangle} t_{ij} c_i^\dagger c_j \tag{4.1}$$

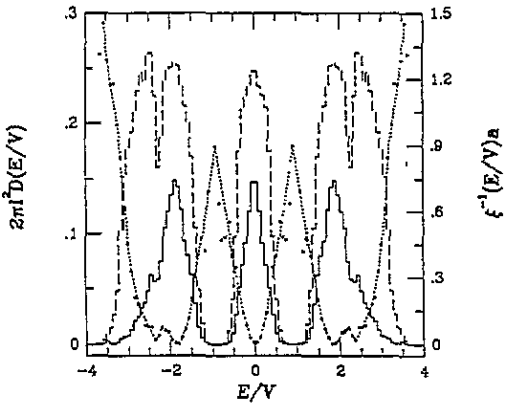

Figure 4. The sample averaged density of states (broken line) and density of current-carrying states (full line) are plotted for $V_1/V = 0.2$ and $q/p = \frac{2}{5}$. The full dots show the rescaled inverse localization length $\xi^{-1}(E/V)a$, whose scale is shown by the right y axis. a is the period of the periodic potential.

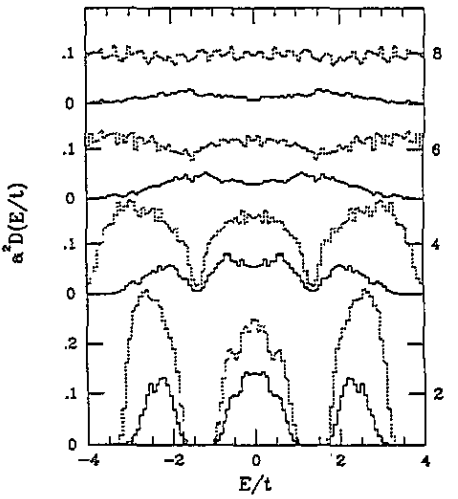

Figure 5. The histogram of the sample averaged density of states (dotted line) and density of current-carrying states (full line) is shown for tight-binding electrons in a magnetic field given by $q/p = \frac{1}{3}$. The numbers on the right-hand side show the degree of disorder, namely W/t. The total density is normalized to one particle per unit cell.

where $\langle ij \rangle$ refers to the nearest neighbours. ϵ_i is the site energy, which is a random number between $-\frac{1}{2}W$ and $\frac{1}{2}W$ with a uniform probability of $1/W$. The effect of the magnetic field is introduced by the Peierls substitution,

$$t_{ij} = t \exp\left(\mathrm{i}\frac{2\pi}{\phi_0}\int_i^j \boldsymbol{A}\cdot \mathrm{d}\boldsymbol{l}\right). \tag{4.2}$$

The square lattice and the Landau gauge are chosen. The magnetic flux through each unit cell is $\phi/\phi_0 = q/p$, where the notation used in section 2 has been reversed for convenience. The periods of random site energy are L in both directions. L should be an integer multiple of pa where a is the period of the lattice. This defines a finite $L^2 \times L^2$ matrix.

If one writes the solution

$$\psi_{n,m} = \exp(\mathrm{i}k_1 n + \mathrm{i}k_2 m)u_{n,m} \tag{4.3}$$

where n, m are discrete labels of lattice sites, the effective hopping term, with respect to $u_{n,m}$, becomes

$$\tilde{t_{ij}} = t_{ij}\exp[\mathrm{i}\boldsymbol{k}\cdot(\boldsymbol{j}-\boldsymbol{i})]. \tag{4.4}$$

Similarly, the velocity operator can be written as the partial derivative of the Hamiltonian with respect to the wavenumbers. Therefore the method described in equations (2.10)–(2.14) is still valid for the calculation of the Hall conductance in this limit. However, in equation (2.13) X' should be the same as X, and equation (2.13) gives an integer multiple of 2π directly. In the absence of disorder, the Hall conductance of the rth band is given by $(s_r - s_{r-1})$ in equation (2.15) instead.

First the sample with a magnetic field given by $q/p = \frac{1}{3}$ is considered. Three bands carry the Hall conductance (1, −2, 1), respectively. L is chosen to be $6a$. There are 36 subbands, each set of 12 subbands forming a band for weak disorder. Similarly, the density of states and the density of current-carrying states are calculated for four values of $W/t = 2,\ 4,\ 6$ and 8. Figure 5 shows the result where 100 samples have been averaged. When the sign of all the site energies is reversed, the Hall conductance and density of states can be obtained from the previous results simply by reversing the energy. This is because the site energies are the only diagonal elements and the hopping terms give a symmetric spectrum about zero energy. When disorder is introduced, the current-carrying states in the central band, which carry −2 Hall currents, split into two, each carrying −1 Hall current. As disorder increases, they merge with those in neighbouring bands which carry 1 Hall current. Then two (1, −1) pairs are formed and annihilated for a larger degree of disorder.

It is not surprising that one finds a similar pattern for $q/p = \frac{2}{5}$. The Hall conductance for each band is (−2, 3, −2, 3, −2), respectively. The Hall conductances for eight values of W/t are shown in figure 6(A) when $L = 5a$, and the corresponding density of current-carrying states is shown in figure 6(B). For $W/t = 0.8$, the Hall conductance of 1 in the second band has been annihilated with that of −1 in the first band, and similarly for the fourth and fifth bands. As disorder further increases, for example $W/t = 1.9$, two Hall currents in the second band split. For $W/t = 3.2$, the current-carrying states in the central band start to split. Now this is similar to the case of $q/p = \frac{1}{3}$, except there is a (1, −1) pair which has not been annihilated in this sample.

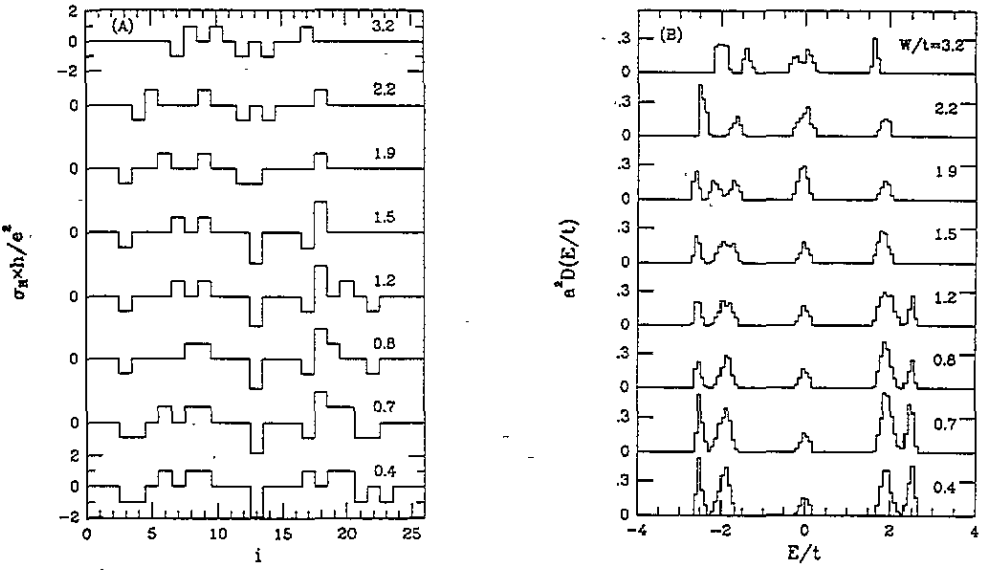

Figure 6. The calculated Hall conductance for one sample is plotted in (A) against the subband index i for eight values of W/t and $q/p = \frac{2}{5}$. The corresponding density of current-carrying states (full line) is drawn in (B).

Finally, the localization properties in this limit are also investigated. Similarly based on the Thouless number method, numerical calculations have been made of the localization length for $q/p = \frac{1}{3}$. Two sizes with $L = 15a$ and $18a$ are considered. The results are shown

in figure 7. For $W/t = 3$, singular energies in the lower and upper bands are observed to carry the currents. However, the localization in the central band, where the Hall currents of 2 appear, seems to be suppressed. A finite region of energy may be occupied by extended states. For $W/t = 5$, the gaps have vanished, and an even wider region of extended states emerges. In this case, there are two $(1, -1)$ pairs. It is resonable to expect the same features in the previous limit of split Landau levels, for example for $q/p = \frac{3}{5}$ and weak disorder the second and fourth bands carry two Hall currents. Further considerations, for example using one-parameter scaling theory, may possibly shed light on this problem.

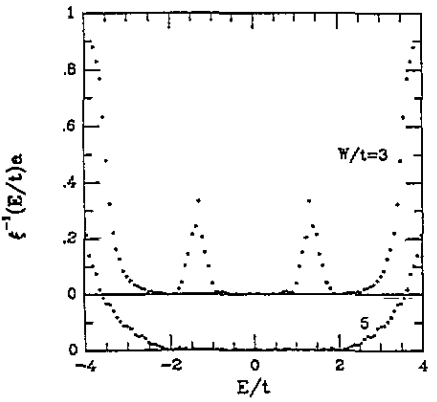

Figure 7. The rescaled inverse localization length $\xi^{-1}(E/t)a$ is plotted as a function of rescaled energy E/t for $q/p = \frac{1}{3}$ and $W/t = 3,\ 5$.

5. Proposed phase diagrams

The above results can be summarized to give a phase diagram, where the locations of current-carrying states in the energy space are shown as a function of disorder. Figure 8(A) shows the diagram for split Landau levels. Starting with the flux $p/q = \frac{8}{5}$, there are eight bands with two central ones touching at zero energy. The first three bands carry the Hall currents (2, −3, 2), respectively, and similarly (2, −3, 2) for the last three. The two central bands carry 1 Hall current in total. Without disorder, the Hall currents are carried by the entire band. As disorder is introduced, extended states appear only in a region around the critical energies in each band. The critical energies in the Hofstadter spectrum are defined where the density of states diverges logarithmically. As mentioned in the last section, it is possible that these regions have finite widths if $|\sigma_H| > 1$. However, it has been assumed that these regions are actually singular energies. The corresponding modification can be easily made if indeed these regions have finite widths. For a certain degree of disorder, for example above the broken line in figure 8(A), the diagram is similar to that for $\phi = p/q = \frac{5}{3}$. When disorder is further increased above the broken line, the diagram takes the shape of $\phi = p/q = \frac{3}{2}$. The diagrams for other sequences of p/q can be generated similarly.

The diagram for the tight-binding electrons is plotted in figure 8(B). The flux is chosen to be $\phi = q/p = \frac{2}{5}$, where the Hall currents are (−2, 3, −2, 3, −2) for each band. For sufficiently strong disorder above the broken line, the diagram of $q/p = \frac{1}{3}$ is reproduced.

These two diagrams are qualitative ones. The accurate values of disorder where annihilation occurs can be obtained from numerical calculations.

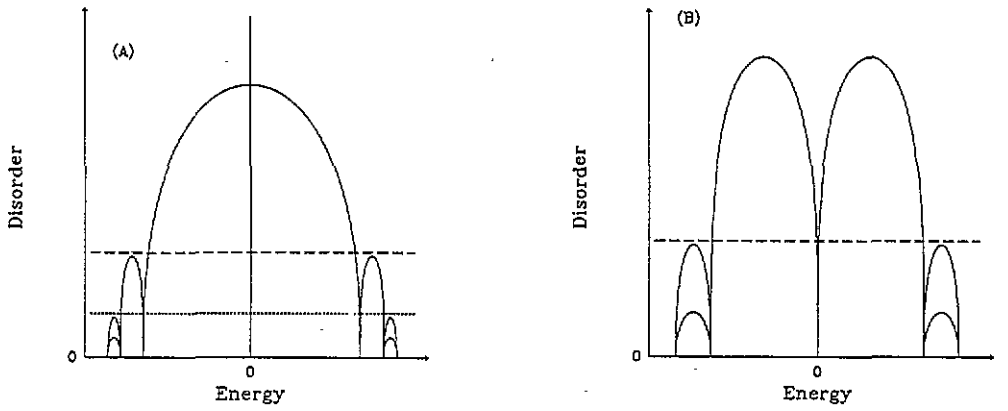

Figure 8. The proposed phase diagrams are drawn for the split Landau levels in (A) with the flux $\phi = p/q = \frac{8}{5}$, and for tight-binding electrons in (B) with the flux $\phi = q/p = \frac{2}{5}$.

6. Conclusions

In this paper, two-dimensional electrons subject to a magnetic field and simultaneously modulated by a periodic potential have been studied in the presence of disorder. Numerical calculations have been made of the Hall conductance for two limiting cases which generate the Hofstadter spectrum. The Hall conductance is obtained by the total phase change of the wavefunction when a contour is taken along the boundary of the unit cell in wavenumber space. This study has been focused on how the structure of Hall conductance changes with disorder.

In section 2, the limit where the Landau level is perturbed by a weak periodic potential is considered. Two fractions of the flux are calculated. For $\phi = \frac{3}{2}$, the lower and upper bands both carry 1 Hall current. As disorder is increased, the gaps start to shrink and the current-carrying states in the lower and upper bands move towards the central band where -1 Hall current is carried. For sufficiently strong disorder, the gaps vanish and there is only 1 Hall current carried at the centre of the broadened Landau level. For $\phi = \frac{5}{3}$, there are two bands carrying 2 Hall currents. As disorder is increased, the states carrying 2 Hall currents will split into two with each carrying 1 Hall current, one of which will merge and annihilate with that in the neighbouring band carrying -1 Hall current. For a certain degree of disorder, the structure of Hall conductance becomes similar to that of $\phi = \frac{3}{2}$.

In section 3, the localization length has been obtained by using the Thouless number method. It has been observed that the Hall current is still carried by a singular energy in a band if the Hall conductance is either 1 or -1. Based on this, it is concluded that a plateau can be measured as a function of magnetic field for one-third filling of Landau levels.

In section 4, the opposite limit is studied where the periodic potential dominates. The system is described by the tight-binding model with random site energies. The formulae used in section 2 are still applicable when minor modifications are made. The splitting and annihilation of Hall current-carrying states are also observed. There is also a calculation of localization length. But it is not conclusive whether extended states locate at singular energies if a band carries higher Hall currents or if there is a $(1, -1)$ pair. The possibility of mobility edges needs to be further investigated.

The results obtained in sections 2 and 4 are summarized in section 5 to propose qualitative diagrams, where the flow of extended states with disorder is demonstrated clearly.

Acknowledgments

I am very grateful to Professor David Thouless for his valuable advice and constant encouragement during my graduate study. I must thank him for sharing with me his original ideas on this work. I would also like to thank Q Niu, P Ao, M den Nijs and B Spivak for useful discussions. This work was supported in part by the National Science Foundation under Grant No DMR-9220733.

References

[1] von Klitzing K, Dorda G and Pepper M 1980 *Phys. Rev. Lett.* **45** 494
[2] Abrahams E, Anderson P W, Licciardello D C and Ramakrishnan T V 1979 *Phys. Rev. Lett.* **42** 673
[3] Halperin B I 1982 *Phys. Rev.* B **25** 2185
[4] Trugman S A 1983 *Phys. Rev.* B **27** 7539
[5] Mil'nikov G V and Sokolov I M 1988 *Pis. Zh. Eksp. Teor. Fiz.* **48** 494 (Engl. transl. *JETP Lett.* **48** 536)
[6] MacKinnon A and Kramer B 1981 *Phys. Rev. Lett.* **47** 1546; 1983 *Z. Phys.* B **53** 1
[7] Huckestein B and Kramer B 1990 *Phys. Rev. Lett.* **64** 1437
[8] Aoki H and Ando T 1985 *Phys. Rev. Lett.* **54** 831
Ando T and Aoki H 1985 *J. Phys. Soc. Japan* **54** 2238
[9] Ando T 1983 *J. Phys. Soc. Japan* **52** 1740
[10] Thouless D J, Kohmoto M, Nightingale M P and den Nijs M 1982 *Phys. Rev. Lett.* **49** 405
[11] Niu Q, Thouless D J and Wu Y S 1985 *Phys. Rev.* B **31** 3372
[12] Kohmoto M 1985 *Ann. Phys., NY* **160** 343
[13] Aoki H and Ando T 1986 *Phys. Rev. Lett.* **57** 3093
[14] Arovas D P, Bhatt R N, Haldane F D M, Littlewood P B and Rammal R 1988 *Phys. Rev. Lett.* **60** 619
[15] Huo Y and Bhatt R N 1992 *Phys. Rev. Lett.* **68** 1375
[16] Harper P G 1955 *Proc. Phys. Soc.* A **68** 874
[17] Hofstadter D R 1976 *Phys. Rev.* B **14** 2239
[18] Středa P 1982 *J. Phys. C: Solid State Phys.* **15** L1299
[19] Ando T 1988 *Surf. Sci.* **196** 120
[20] Edwards J T and Thouless D J 1972 *J. Phys. C: Solid State Phys.* **5** 807
[21] Licciardello D C and Thouless D J 1975 *J. Phys. C: Solid State Phys.* **8** 4157
[22] Ando T 1992 *Surf. Sci.* **263** 137
[23] Fang H and Stiles P J 1990 *Phys. Rev.* B **41** 10 171
[24] Gerhardts R R, Weiss D and Wulf U 1991 *Phys. Rev.* B **43** 5192
[25] Ismail K, Smith T P III, Masselink W T and Smith H I 1989 *Appl. Phys. Lett.* **55** 2766
[26] Gerhardts R R and Pfannkuche D 1992 *Surf. Sci.* **263** 324
[27] Tan Y 1994 *Phys. Rev.* B **49** 1827
[28] Thouless D J 1984 *J. Phys. C: Solid State Phys.* **17** L325